ELSEVIER

Journal of Molecular Structure: THEOCHEM 773 (2006) 43–52

THEO CHEM

www.elsevier.com/locate/theochem

Electronic structure of dimetallocene molecules: Dizincocene $Zn_2(\eta^5\text{-}C_5Me_5)_2$

Michael R. Philpott [a,b,*], Yoshiyuki Kawazoe [a]

[a] *Institute for Materials Research, Tohoku University, 2-1-1 Katahira, Sendai 980-8577, Japan*
[b] *Department of Materials Science, Faculty of Science, National University of Singapore, Singapore 117543, Singapore*

Received 21 April 2006; received in revised form 26 June 2006; accepted 27 June 2006
Available online 10 July 2006

Abstract

The properties of the recently synthesised dizincocene $Zn_2(\eta^5\text{-}C_5Me_5)_2$ have been studied by *ab initio* calculations using plane wave based density functional theory. The calculated geometry agrees well with single crystal X-ray measurements. Every methyl group is similarly oriented with one CH bond pointed away from the core approximately in a plane containing the configuration axis. The C_5Me_5 ligand is dished outwards. The Zn–Zn axis is not quite perpendicular to or pointed exactly at the C_5 ring centers. The top and bottom C_5 rings are not parallel but tilted a few degrees with respect to each other. In the central Zn–Zn bond there is less charge, indicated by isometric total charge density surfaces, than between ligand and metal atom. This metal–metal bond has σ- and π-components with the σ-bond mainly s-, with small p_z- and d_{z^2}-components and the π-bond with p_x-, p_y-, d_{zx}-, d_{yz}-components. The π^*-lumo orbital is especially interesting because the excited state charge is confined to a disk-like shape because of Pauli repulsion from the methyl groups. The electron localization function (ELF) has distinctive features. In the region of the dizinc central bond, the valence basin has toroidal and central ellipsoid components (ELF > 0.5) found in the zincous dication Zn_2^{2+}. The valence basins of the C–C bonds of the C_5 ring are displaced slightly parallel to the major axis away from the central region, this effect along with geometric dishing is tentatively assigned as due to a small change in hybridization of ring carbon atoms due to loss of aromaticity.

Keywords: Dizincocene; Zincous ion Zn_2^{2+}; Quantum electronic structure; Density functional theory; Electronic structure; Electron localization function ELF; Partial charge density; Kohn–Sham level

1. Introduction

Molecules with multiple rings connected axially to small clusters of metal atoms are of interest for nano-mechanical components, molecular electronics circuit elements, and catalytic systems for inert gas reductions in synthetic applications. This paper summarizes an *ab initio* plane wave density functional theory (DFT) quantum study of the geometrical structure and the electronic properties for one such system, namely the recently synthesized dimetallocene $Zn_2(\eta^5\text{-}C_5Me_5)_2$ [1,2]. This molecule is unusual in having two zinc atoms 230.5 pm apart sandwiched between pentamethyl cyclopentadienyl (henceforth $Cp^* = C_5Me_5$) ligands in an orientation with axis very nearly perpendicular to the rings. The Zn–Zn distance is quite short compared to the solid metal nearest neighbor distance 266 pm [3]. The molecule can be considered as arising from the zincous Zn_2^{2+} ion which would, if it existed independently, be a lower atomic number analog of the well characterized and chemically stable group twelve mercurous ion Hg_2^{2+} [4,5]. The chemistry of the zincous dication is interesting, there is no resemblance to neutral group 12 dimers which are weakly bonded and are better considered as van der Waals complexes and not covalently bonded molecules [6] because their atomic configuration is $(n-1)d^{10}ns^2$. However, when electrons are donated to exterior ligands

* Corresponding author. Present address: 1631 Castro Street, San Francisco, CA 94114, United States. Tel.: +1 415 824 7557.
E-mail address: philpott@imr.edu (M.R. Philpott).

0166-1280/$ - see front matter © 2006 Elsevier B.V. All rights reserved.
doi:10.1016/j.theochem.2006.06.040

then the formation of a covalent metal–metal bond becomes possible and an ionic model would be $M_2^{2+}(L)^2$. Back donation from ligand to metal would offset and reduce the nuclear Coulombic interaction. One signature of ligands capable of resupplying charge to the metal would be a shortening of the Zn–Zn bond and this is a key property of the dizincocene molecule. Indeed the metal–metal bond distance in the isoelectronic Cu_2 ($S = 0$) dimer is 222 pm when calculated by exactly the same method as used here compared to 246 pm for the isolated zincous Zn_2^{2+} ion [7]. Electron transfer to the cyclopentadienyl radical Cp ($Cp = C_5H_5$) and Cp^* is facilitated by aromatic stabilization energy. Some rebalancing of charge distribution through back donation into metal d-orbitals would contribute to partial neutralization of the central metal atoms and a concomitant reduction in total energy of the molecule.

The themes followed in this work are:

- modification of the levels in the Zn_2^{2+} core by the attached ligand Cp^*;
- study of the contribution from s-, p- and d-functions to the Zn–Zn and the Zn-ligand bonds;
- alteration of the structure of the Cp^* ligand.

In this work we use a plane wave basis DFT method with periodic boundary conditions. The plane wave energy cut-off controls adequacy and accuracy of the wavefunction and charge density. We calculate total charge density, partial charge density plots of the Kohn–Sham (KS) levels and the electron localization function (ELF). The definition of ELF is that introduced by Becke and Edgecombe [8] and Silvi and Savin [9] and subsequently by many other groups. These properties were found to be useful in interpreting the nature of the chemical bonds found in dimetallocenes in particular the metal–metal bond and its pendant orbitals. Our application of ELF is qualitative and not precise, which would require single point calculations with an all electron wavefunction. Nevertheless this application is both useful and insightful. Confidence in this position is the result of unpublished calculations of the ground and first triplet state of about thirty organic molecules and some small inorganic molecules. The ELF of the molecules matched the valence features of those all electron calculations of which we are aware.

The definition of the ELF follows Becke and Edgcombe [8].

$$\mathrm{Elf}(\mathbf{r}) = \{1 + [D(\mathbf{r})/D_\mathrm{h}]\}^{-1} \tag{1}$$

$$D(\mathbf{r}) = 1/2\sum_i |\nabla\varphi_i(\mathbf{r})|^2 - 1/8|\nabla\rho(\mathbf{r})|^2/\rho(\mathbf{r}) \tag{2}$$

$$D_\mathrm{h} = (3/10)(3\pi^2)^{5/3}(\rho)^{5/3} \tag{3}$$

Here $\rho(\mathbf{r}) = \sum_i \rho_i(\mathbf{r})$ is the total electron density and $\{\varphi_i(\mathbf{r})\}$ ($i = 1, \ldots, N$) are a set of KS orbitals making up a single determinant wavefunction and $\rho_i(\mathbf{r})$ is the partial charge density assigned to the ith KS level. Briefly electron localization occurs in regions where elf >0.5 and delocalization where elf <0.5.

During the course of this work several papers have appeared [2,10–16] addressing aspects of dimetallocene structure which were also stimulated by the work of Carmona et al. [1,2]. These calculations reveal some interesting aspects of dimetallocenes with Cp, Cp^* and more complex ligands for metals Zn, Cd, Cu, Ni, Ca, Be, Mg. We briefly comment on this previous work to bring context to the present study. The paper by del Rio et al. [2] was concerned with confirming the findings of the crystal structure analysis for example the short metal–metal bond distance and the absence of H atoms in the dimetal core. The main topic of the paper by Xie et al. [10] was concerned with the structure of non transition dimetallocenes with Be, Mg and Ca cores and not dizincocene. In Xie et al. [11] the topic was the structure of singlet (parallel to rings) and triplet (perpendicular) states of Cu and Ni dimetallocenes. For comparison a discussion of the structure of the dizincocene Zn_2Cp_2 was included. Xie et al. [12] discussed the structure of several group 12 (Zn, Cd) dimetallocenes. Kang [13] used plane wave DFT method studied the structure of Zn and Cd dimetallocenes including compounds with larger ring systems than Cp and Cp^*. In the paper by Kress [14] the geometry and the vibrational modes with frequencies greater than 92 cm^{-1}, were described. The paper by Timoshkin and Schaefer [15] describes donor–acceptor sandwich of main group elements and the paper by Richardson et al. [16] discusses possible vibrational signatures in the dizincocene molecule.

In this paper we focus attention on interesting details of the geometry (Cp^* ring dishing, off-center positioning of metal atoms, tilt of the Cp rings) not heretofore fully discussed, electronic structure using total charge, KS level partial charge densities and the ELF. We consider also the influence of the packing of the dizincocene molecules in the crystal and how this environment could affect the geometry of the molecule.

This paper is organized as follows. Section 2, describes in outline the computational details and briefly the advantages and disadvantages of the methodology used in this paper. Section 3 describes the results of the calculations starting with geometry including a discussion of the crystal geometry, then moving to total charge, homos–lumos and ELF.

2. Computational method

The calculations were performed using VASP, an *ab initio* ultra-soft pseudo-potential plane wave methodology with the spin polarized generalized gradient approximation for the exchange-correlation energy [17–23]. The exchange-correlation functional, parameterized by Perdew et al. [17,18], was used with the generalized gradient approximation. The plane wave high energy cut-off (394 eV) was chosen higher than the maximum for the set of pseudopotentials used to facilitate smooth ELF. The

calculations were performed using periodic boundaries with a cubic cell, edge length 1.5 nm. All Brillouin zone integrations were done at the gamma point. The highest point group symmetry available in these calculations was D_{4h}. The geometry was optimized using the conjugate gradient method. In these calculations the residual forces acting on each atom were equal to or less than about 10 μeV/pm (0.8 cm^{-1}/Å). Analysis of charge densities was done in several ways: By integrating density inside spheres surrounding each atom with a radius was taken to be half or just greater than one half of the nearest neighbour distance; projecting the wavefunction inside the same spheres onto the spherical harmonics (l, (m)) corresponding to s, p(p_x, p_y, p_z) and d (d_{xy}, d_{yz}, d_{zx}, d_{z^2}, $d_{x^2-y^2}$) functions for each atom; calculating isometric surfaces for total charge and partial charge associated with selected Kohn–Sham (KS) levels; calculating isometric surfaces of the ELF density. In the geometry optimizations the Cp^* ligands were started off staggered, eclipsed and intermediate relative orientations. In the final stage the symmetry constraints were relaxed.

Size of the simulation box was deemed adequate. The dizincocene molecule corresponded to a cylinder with length times diameter equal to 850 pm × 655 pm. In the periodic lattice (1.5 nm cell edge) the hydrogen atoms in different cells were 650 pm or more apart and all other atoms 850 pm apart. Accordingly the molecules in these calculations are quite well separated and outside the overlap of van der Waals radii for carbon and hydrogen. This point is relevant for the discussion of differences between theory and experiment since the actual dizincocene crystal (triclinic) has a space efficient packing arrangement with numerous H–H contacts.

The use of a colour scale to visualize and interpret density features is very useful in interpreting chemical bonding. In the linear scale the data is mapped into the range 0–1, and assigned a color (blue = 0, red = 1) to each value in this range. For the logarithmic scale the data is first scaled linearly into the range 1–e^2, and then the natural log of the resulting value is taken, and divided by 2, to provide a number between 0 and 1, which is then assigned a color. The electron density maximum, denoted d_{max} in the scales has the value given in the text or in the figure caption. The value of density plotted as an isometric surface is denoted d_{iso} in the text or in the figure caption.

3. Dizincocene $Zn_2(\eta^5\text{-}C_5(CH_3)_5)_2$

The calculations were performed in two stages. Generally we started with a model geometric configuration that had a high symmetry (e.g., D_{5h} eclipsed or D_{5d} staggered). The crystal structure geometry [1,2] was not used. We also ran calculations with an intermediate low symmetry C_1. Standard molecular modeling software was used to create the geometry with standard bond lengths and flat Cp^* ligands. In the second stage we relaxed symmetry requirements. The total energies were always similar (within 0.1 eV) provided the methyl groups were oriented such that one C–H bond on each methyl was pointed away from the dimetal core and approximately in the plane defined by the two metal atoms and the C atom of the methyl group. A sense of this orientation of C–H bonds can be seen in Fig. 1 which shows the result of a calculation that started from a fully eclipsed conformation with no symmetry imposed in the later part of the calculation. As mentioned above the differences in total energy of isolated dizincocenes in different configurations involving eclipsed and staggered as extremes were found to be small, less than 0.1 eV, and will not be discussed further, except to comment that the rotation of the Cp^* rings has low thermally accessible barriers. For definiteness we limit discussion to results from calculations started from an eclipsed conformation. Fig. 1 shows an eclipsed conformer with the labeling on the C atoms discussed in text. For clarity the two zinc atoms are not labeled. Zn1 is attached to the top Cp^* and Zn2 to the lower Cp^*. The atom labels are: Zn atoms: 1, 2 (not shown in Fig. 1); C atoms: upper C5 ring labels C3–C7; upper CH_3 groups labels C13–C17; lower C5 ring labels C8–C12; lower CH_3 group labels C18–C22.

3.1. Geometry

Table 1 summarizes the computational results and compares them with the geometry adapted from the published

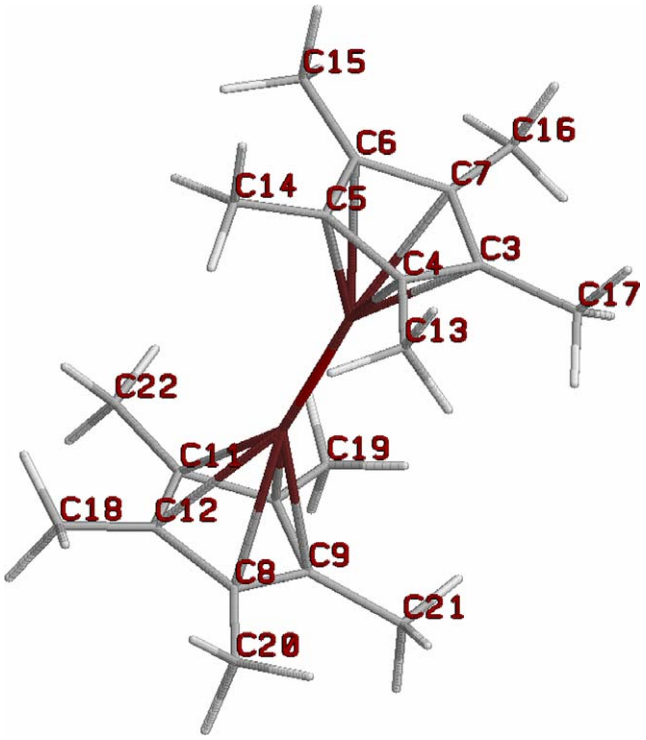

Fig. 1. Wire frame model of dizincocene $Zn_2Cp^*_2$ with Cp^* units in a near eclipsed conformation based on calculated geometry initially starting from an eclipsed conformation. Labels on the C atoms are those used in text. For clarity the two zinc atoms are not labeled. Zn1 is attached to the top Cp^* and Zn2 to the lower Cp^* unit. Note orientation of methyl groups with one CH bond approximately parallel to the molecular long axis.

Table 1
Comparison of calculated and experimental geometry parameters[a]

Parameter	Calculation	Experiment [1,2]
Zn1–Zn2	228.5	230.5
All C–H	110	97.8–98.1
Zn–C upper Cp*	226–229	227.5–229.5
C–C upper	143	142–143
C–CH_3 upper	149	150–151
C5 upper-C5 lower	605–608	615–619
CH_3 upper –CH_3 lower	620–643	632–647
Ring <C–C–C upper	107.80–108.13	107–108
<CH_3–C–C upper	Av 125.83 (125.47–126.08)	125–127
<H–C–C upper	107.71–108.31	Av 109.5

[a] Distance/pm, angle/deg.

crystal structure data [1,2]. We start with a description of the general shape of the molecule. Our calculations show that the Zn–Zn axis is not exactly perpendicular to the planes of the two Cp* ligands. In addition the Cp* rings are dished outwards and tilted relative to an axis joining the ring centers. Though these are small effects the published crystal structure shows these trends [1,2]. The stick bond framework joining atoms inside the isometric surface Fig. 2 for the total charge density shows the dishing of the Cp* rings in which the C atoms of the methyl groups are shifted away from the dimetal core region. Dishing of pentamethyl- and tetramethyl-substituted cyclopentadienyl ligands can be seen in published crystal structures [22] of other monometallocene complexes. Computational evidence of dishing in M_2Cp_2 with the simpler Cp ligand is a much smaller effect. In their interesting paper Xie et al. [12] showed but did not comment on positive dishing for dizinconene and negative dishing in the triplet state of dinickelocene. The methyl groups are rotated such that one H atom on each methyl is pointing away from the central core roughly in a plane which contains the Zn–Zn axis. The five carbons making up the C_5 ring lie on a plane, likewise for the C atoms of the five methyl groups. These planes through the C atoms of C_5 ring and the five CH_3 groups have a small relative tilt of approximately 2–3°. Torsion angle measurements of the calculated geometry indicate that in the Cp* ligand the C_5 ring and the 5-ring of C atoms making up the methyl groups are essentially flat. At best the torsions show deviations from planarity of less than 1°. The methyl groups are positioned in a plane further from the dimetal core than the C_5 ring. The torsion angles H_3C–C_5–C_5–CH_3 were found to be not greater than approximately 3°, which agrees with the observation that Cp* is dished. Starting with the eclipsed conformation and running without symmetry constraints showed that the Cp* rings had a relative rotation of were rotated relative to each other about the Zn–Zn axis by approximately 2–3°.

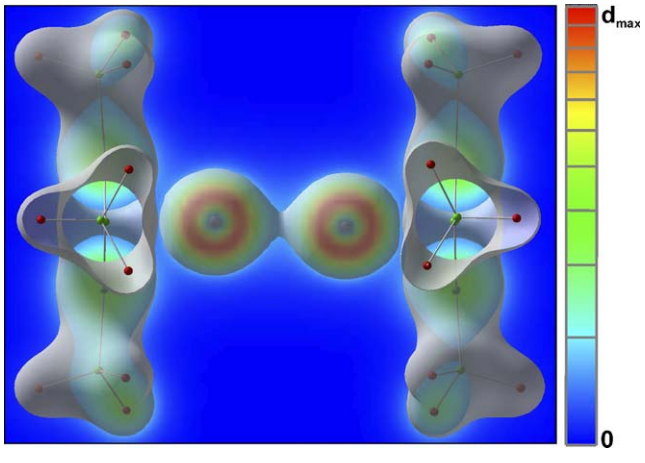

Fig. 2. Total charge density (colour log scale) on a plane through the zinc atoms, maximum density $d_{max} = 24910$ (red). Superimposed is an isometric density surface for $d_{iso} = 1470$ corresponding to enclosure around zinc atoms. The surface enclosing the Cp* ligands corresponds to $d_{iso} = 5040$ and the entire molecule is enclosed at approximately $d_{iso} = 1000$. Wire frame bond model for the Cp* ligands shows outward dishing described in text. Each methyl group has one C–H bond oriented approximately parallel to the molecular long axis. (For interpretation of the references to colour in this figure legend, the reader is referred to the web version of this article.)

The regular pentagon has an internal <C–C–C bond angle equal to 108°. For the calculated bond angles we found that the internal Cp* bond angle <CCC = 107.80–108.13° (C_5 rings). For the corresponding angle involving the C atom of the CH_3 group the angle <CCC = 107.71–108.31. These carbon atoms are not bonded. Relative tilt of the Cp* rings comes from the calculated C(upper ring)–C(lower ring) distances. For the "eclipsed" atoms the x and y-coordinates are very similar. Therefore the distances listed next are almost the same as the difference in z-coordinate. Distances between "pairs" of C atoms in the C_5 rings are in the range 608–618 pm. These distances were used to calculate approximately the relative tilt of the two Cp* moieties to be a few (2–3) degrees. Overall agreement between theory and experimental geometry is good. Table 1 demonstrates that the deviations from planarity, orthogonality and symmetry occur in the crystal though not quite so large. We postpone further discussion of this topic to Section 3.2 where the discussion is enlarged to consider the packing of dizincocene molecules in the crystal lattice.

3.2. Total charge density

Fig. 2 shows a 2D log scale colour density plot ($d_{max} = 24{,}910$) with a superimposed 3D isometric surface plot ($d_{iso} = 1470$) of the total charge density. The 2D plane slice cuts through the Zn atoms and the filled zinc 3d shell is clearly visible. The isometric surface has three unconnected regions, two enclosing the ligands and one enclosing both metal atoms. The density d_{iso} corresponds approximately to the highest charge density in the metal–metal. This isometric surface density is much lower than densities inside C–H and C–C bonds or for that mater the highest density enveloping the Cp* ligand ($d_{iso} = 5040$). The entire molecule, zinc atoms and Cp* ligands, is enclosed in a single surface corresponding at $d_{iso} \approx 1000$. For isosurfaces

with high d_{iso} values the development of C–H and C–C bonding within each Cp^* ligand was readily followed. Charge density spreads along paths connecting atoms for simple σ-bonds and spreads laterally also (perpendicularly to the plane of the rings) for the σπ-bonds connecting the atoms of the C_5 ring. In this molecule there is no hint, in the total charge density or its manifold of isometric surfaces or in the ELF density, of directed atom–atom bonding in the space between Zn and Cp^*. To see structure in the charge density in this region we have to resolve the total charge in to separate partial charge densities of the occupied Kohn–Sham levels.

3.3. Partial charge densities

Electronic charge can be probed more deeply in two ways. First we present in Tables the projection of the total system wavefunction onto harmonic functions inside a sphere of given radius for the most important occupied KS levels (homos). The atomic sphere radii were 125 pm for Zn and C atoms and 75 pm for H atoms. Although these radii are a little larger than half the atom–atom bond distances and so the numbers capture contributions in the greater environment and they are nevertheless useful. Second we plot the partial charge density of individual KS levels on plane slices through the molecule and also as 3D isometric surfaces just as we did for the total charge density.

The KS level 62 and those lying deeper (energies $\leqslant -7.25$ eV) are made up of deep lying π- and σ-levels of the C–C bond frame work of the Cp^* ligands or isolated d-levels of the Zn atoms, and will not be described further. The KS levels 63–67 have energies in the range $E = -5.355$ to -4.1323 eV. This group of five highest occupied levels (homos 1–5) are responsible for all of the bonding between Zn atoms and from Zn to the Cp^* ring carbon atoms. The homo-1 (KS 67) and -2 (KS 66) describe a state with bonding between Cp^* and Zn and no bond between the Zn atoms. Levels (KS 65–64) homo-3 and homo-4 correspond to π-like bonding between several C atoms of Cp^* and a Zn atom and to weak pi-bonding between the Zn atoms. Homo-5 (KS 63) corresponds to σ-bond between the Zn atoms. We describe the characteristics of each briefly below. Also examined are the lowest unoccupied KS levels (lumos 1–3) because their charge distributions suggest there are low lying $S = 0$ excited electronic states in which the charge is confined by Pauli repulsion from the methyl groups.

Fig. 3 shows the partial charge density associated with the highest occupied Kohn–Sham (KS) level 67, homo-1, $E = -4.132$ eV. Table 2 shows the projection of the wavefunction on to harmonics ($l = 0, 1, 2$) inside a sphere radius 125 pm centered on Zn and C atoms. Atoms with identical projections are omitted (e.g., Zn2 and all C atoms in the lower Cp^* ligand) as well as all H and methyl group C atoms. In addition d-functions not contributing (δ-functions: d_{x^2}, d_{xy}) in the energy range of the homos considered

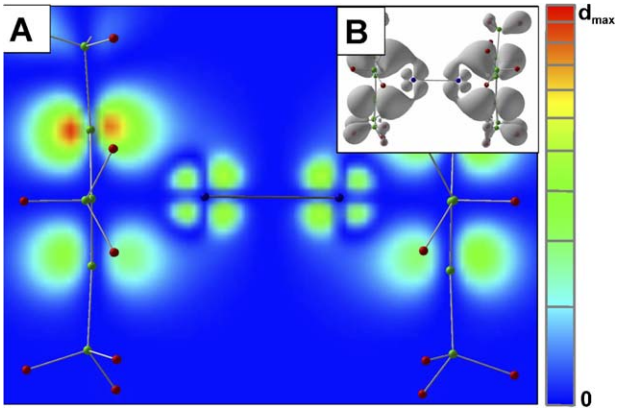

Fig. 3. Plot of the partial charge density for homo1, KS 67, $E = -4.132$ eV on a plane through zinc atoms. Density maximum $d_{max} = 1263$ (red) and $d_{iso} = 30$ (inset). This level which is bonding between Cp^* and the nearest Zn but not bonding for the zinc atoms consists of π-type overlap between C atom p_z-functions and p- and d-functions centered on the Zn atoms in an "over the top motif" described in text and shown more clearly in the inset. (For interpretation of the references to colour in this figure legend, the reader is referred to the web version of this article.)

are omitted. These rules of data reduction apply to all the Tables 2–5. This is a π-type bonding orbital from Cp^* to the nearest zinc atom. The carbon p_z-functions of atoms in the C_5 ring overlap with p- and d-functions centered on the Zn atoms. There is no charge between the Zn atoms so it is not bonding for the metal core. The Zn s-function does not contribute. For spheres of radii (/pm) 125(Zn), 125(C), 075(H), the main components are from zinc p_x which combines with a small contribution from zinc d_{zx} to give a bonding type orbital with the p_z on atoms C4 and C7. The carbon p_z-function overlaps with the interior 3d lobe on the Zn in an "over-the-top" motif seen previously for Cp compounds [24]. There is a node separating charges on the two zinc atoms.

The homo-2 has the same attributes as homo-1 with x and y interchanged and because on the Zn atom it is localized in p_y- and d_{yz}-functions it overlaps two different carbon atoms (carbons C3 and C6) in Cp^*. The energy of homo-2, KS level 66, $E = -4.139$ eV is slightly different due to lower symmetry.

Fig. 4 shows a slice through the partial density of the homo-3 KS level 65, $E = -4.356$ eV. It is a π-type orbital companion almost degenerate in energy with homo-4. This orbital is bonding, it extends over the Cp^*–Zn and weakly to the Zn–Zn central core region. The zinc s-, d_{z^2}-functions do not contribute inside the spheres use to project the wavefunction. The main components of the Zn atom are from the p_x-function which combined with a small contribution from d_{zx}-function to give a bonding type orbital with carbon atoms C4 and C7 which have p_z-functions that overlap with the interior 4p–3d lobe on the Zn atom in the same "an over the top motif" mentioned above and visible in Fig. 4. This Figs. 3 and 4 show the nodal surface through the C atoms of Cp^*.

Table 2
Harmonic projection of wavefunction for Homo-1 (KS 67, $E = -4.132$ eV)

Ion	s	p_y	p_z	p_x	d_{yz}	d_{z^2}	d_{xz}	Total
1	0.000	0.000	0.000	0.014	0.000	0.000	0.020	0.034
3	0.000	0.000	0.001	0.001	0.000	0.000	0.014	0.015
4	0.000	0.000	0.109	0.001	0.003	0.000	0.000	0.113
5	0.000	0.001	0.052	0.000	0.005	0.000	0.004	0.062
6	0.000	0.001	0.033	0.000	0.005	0.000	0.005	0.045
7	0.000	0.000	0.116	0.001	0.001	0.000	0.000	0.119

Table 3
Harmonic projection of wavefunction for Homo-3 (KS 65, $E = -4.357$ eV)

Ion	s	p_y	p_z	p_x	d_{yz}	d_{z^2}	d_{xz}	Total
1	0.000	0.000	0.000	0.025	0.000	0.000	0.008	0.033
3	0.000	0.000	0.001	0.001	0.000	0.000	0.013	0.015
4	0.000	0.000	0.099	0.001	0.003	0.000	0.000	0.104
5	0.000	0.001	0.048	0.000	0.004	0.000	0.004	0.058
6	0.000	0.001	0.031	0.000	0.005	0.000	0.005	0.043
7	0.000	0.000	0.111	0.001	0.001	0.000	0.000	0.115

Table 4
Harmonic projection of wavefunction for Homo-5 (KS 63, $E = -5.355$ eV)

Ion	s	p_y	p_z	p_x	d_{yz}	d_{z^2}	d_{xz}	Total
1	0.116	0.000	0.059	0.000	0.000	0.002	0.000	0.177
3	0.000	0.000	0.020	0.000	0.002	0.000	0.000	0.023
4	0.000	0.000	0.019	0.000	0.000	0.001	0.002	0.021
5	0.000	0.000	0.019	0.000	0.001	0.000	0.001	0.022
6	0.000	0.000	0.020	0.000	0.001	0.000	0.001	0.023
7	0.000	0.000	0.021	0.000	0.000	0.000	0.002	0.023

Table 5
Harmonic projection of wavefunction for Lumo-2 (KS 69, $E = -0.44$ eV)

Ion	s	p_y	p_z	p_x	d_{yz}	d_{z^2}	d_{xz}	Total
1	0.000	0.001	0.000	0.023	0.000	0.000	0.006	0.031
3	0.000	0.000	0.001	0.001	0.000	0.000	0.001	0.002
4	0.000	0.000	0.011	0.000	0.000	0.002	0.000	0.013
5	0.000	0.000	0.002	0.000	0.000	0.000	0.001	0.003
6	0.000	0.000	0.007	0.000	0.000	0.001	0.000	0.009
7	0.000	0.000	0.008	0.000	0.000	0.001	0.000	0.010

Homo-4 is essentially the same as homo-3 discussed above except we interchange x and y as for the first two homos. Homo-4, level 64, $E = -4.362$ eV is a π-type orbital companion to homo-3, in which the contribution is from zinc p_y- and d_{yz}-functions. In this level the zinc atoms engage with carbon atoms C3 and C6 of the Cp^* ligand.

Fig. 5 shows a slice through the metal σ-bonding homo-5 KS level 63, $E = -4.362$ eV, $d_{max} = 820$. There is a vestige of charge density on the axis and an apparent nodal surface running between Zn and Cp^*. The charge is strongly localized between the Zn atoms. Inside the projection spheres see Table 4 the zinc s- and p_z-functions both contribute strongly and are combined with a very small d_{z^2}-component. The zinc π-functions p_x and p_y and other d-functions do not contribute. The low valued d_{iso} isometric surfaces show the ring carbon p_z-functions to be polarized with there main density on the outside of the molecule away from the zinc core and nodal surface through the carbon nuclei of the Cp^* ligand is clearly visible in this case.

Next we briefly comment on some of the lowest unoccupied KS levels (lumo). These auxiliary functions do not contribute to the ground state energy density functional and their properties must be regarded as approximate. The lumo1 KS level 68 energy −0.448 eV describes what appears as a mainly a π-like orbital between the zinc atoms with nodes between the zinc and Cp^* ligands. Lumo1 is a π-bonding orbital which consists mainly of charge on the Zn atoms. There is a small contribution

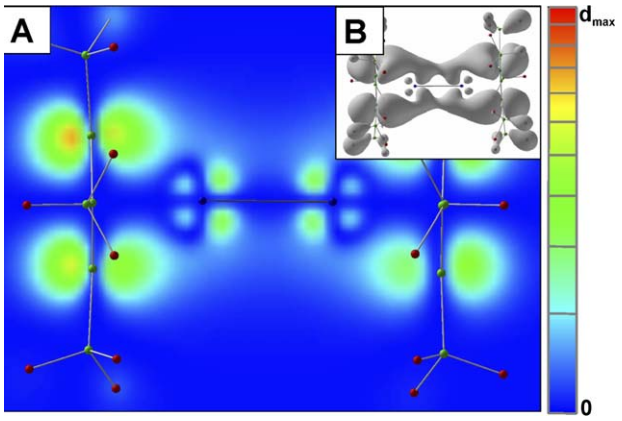

Fig. 4. Plot of the partial charge density for homo3, KS 65, $E = -4.356$ eV ($d_{max} = 1222$ red, $d_{iso} = 25$ inset) on a plane through the zinc atoms. This level is a π-bonding level across the entire molecule. The p_z-functions of carbon atoms C4 and C7 overlap the interior zinc 4p–3d lobe in ''an over the top motif''. (For interpretation of the references to colour in this figure legend, the reader is referred to the web version of this article.)

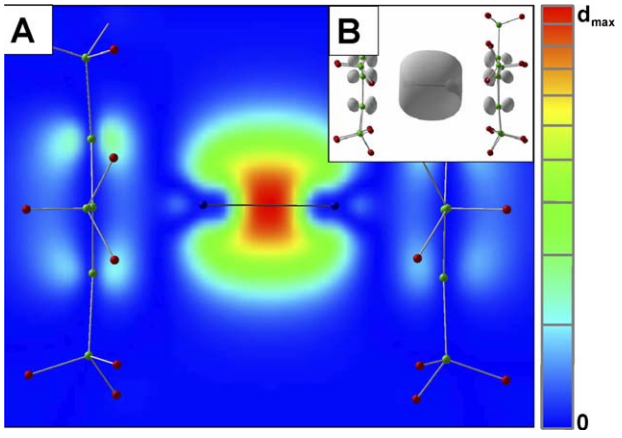

Fig. 5. Plot of the partial charge density for homo5, KS 63, $E = -4.362$ eV ($d_{max} = 820$ red, $d_{iso} = 40$ inset) on a plane through the zinc atoms. This σ-type orbital highly localized between the zinc atoms has very low charge between the Zn and Cp^* ligands. The strongly localized charge between the zinc atoms is contributed approximately evenly by s-, p_z-functions with a very small d_{z^2} component. (For interpretation of the references to colour in this figure legend, the reader is referred to the web version of this article.)

from the Zn 4s-orbital. The main contribution is a zinc p_y-function which combines with a small contribution from zinc d_{yz}-function to give a π-bonding orbital. Fig. 6 shows a slice through the partial charge density for the lumo-2 KS level 69, energy −0.44 eV. There is a node between the zinc partial charge and the p_z charge on the Cp^* units. Lumo-2 is a π-bonding orbital which consists mainly of charge on the Zn atoms. There is no contribution from the Zn 4s-orbital. The main contribution is from the zinc p_x-function which combines with a small contribution from the zinc d_{zx} to give a bonding type orbital. Low values because most of the charge is outside the projection spheres. Note how the charge density is confined to the region between the Cp^* rings. The

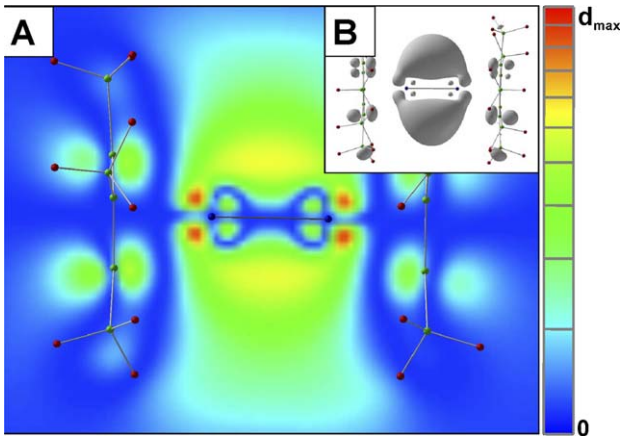

Fig. 6. Plot of the partial charge density for lumo2, KS 69, $E = -0.440$ eV ($d_{max} = 226$ red, $d_{iso} = 50$ inset) as a color log plot (A) and inset an isometric surface (C, $d_{iso} = 50$). This is an excited π-bonding orbital for zinc atoms. There is no contribution from the zinc s-function. Note how the excited charge density is channeled in the region between the Cp^* rings. (For interpretation of the references to colour in this figure legend, the reader is referred to the web version of this article.)

higher lumos appear diffuse and their properties are not considered at all reliable in the calculations reported here.

3.4. ELF

The ELF provides useful information about the bonding in the metal core and within the Cp^* ligands. The highest ELF value is elf = 1.0 (red) and the lowest is elf = 0 (blue). Figs. 7 and 8 illustrate results we have used to investigate the bonding. Wire frame bonds join C atoms (green) and H atoms (red) in the Cp^* ligand and the Zn atoms (blue). Each figure comprises a log colour scale on a planar slice through the molecule with a superimposed 3D isometric surface. In Fig. 7 the plane is through both Zn atoms and in Fig. 8 the plane is perpendicular to and through the mid point of the metal–metal bond. The ELF space partitions into three regions: two separate ligands Cp^*, central Zn–Zn bond and the merged basin enveloping the entire molecule. In Figs. 7 and 8 all the large balloon features are isometric surfaces encompassing the C–H bonds [9] and the smaller egg or cylindrical objects are H_3C–C and C–C bond basins. In Fig. 7A the colour log scale ELF density is projected onto a plane through both zinc atoms. The central yellow-orange feature bisecting the Zn–Zn bond is the 2D plot of the torus and centre spot shown inset (B) in an isometric surface plot (elf = 0.57) which is shown skewed off the metal axis to more clearly display the torus and centre spot features. The arrows connect the torus in Figs. 7A and B. The isometric surface in the main part of Fig. 7 is for elf = 0.75 at which value only features associated with the Cp^* ligands are present.

At lower elf values, ELF basin associated with the Zn–Zn bond appeared as depicted in the inset B of Fig. 7. At elf = 0.592 a ring (torus) centered at Zn–Zn bond center with initial radius 115–130 pm appeared, then at elf = 0.575 the center spot appeared inside the ring and

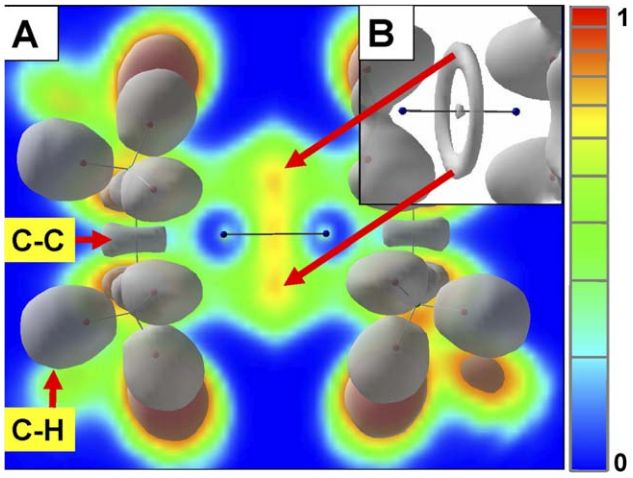

Fig. 7. Colour log scale plot of the ELF on a plane through the zinc atoms. Superimposed an isometric surface for elf = 0.750 showing details of valence C–C bond basins on the ring of the Cp^* ligand. Note the asymmetrical placing relative to the wire frame C–C bond. Large ellipsoid shaped objects are the C–H bond surfaces. Inset a detail of the Zn–Zn region for elf = 0.570 showing the torus and central spot. Log colour scale (blue 0, red 1.0). (For interpretation of the references to colour in this figure legend, the reader is referred to the web version of this article.)

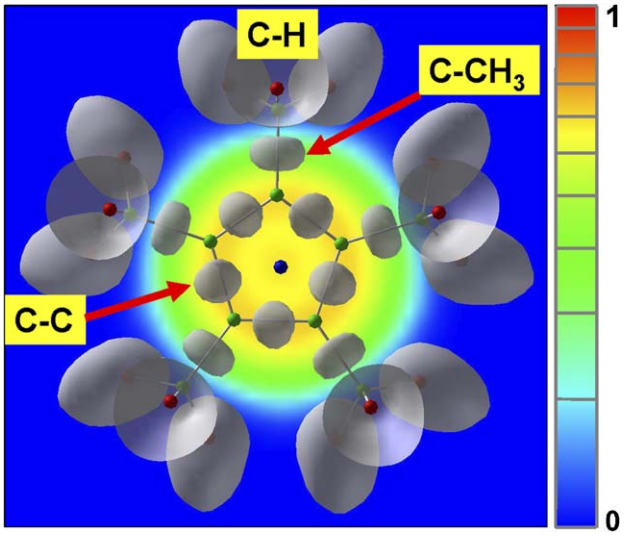

Fig. 8. Isometric surface for elf = 0.750 showing details of valence C–H, $C–CH_3$ and C–C bond basins on the ring of the Cp^* ligand. The $C–CH_3$ basins are symmetrically placed relative to their wire frame bonds whereas the C–C basins are not symmetrically being displaced outward from the ring center. Colour back ground is the ELF value (log colour scale) on a plane through the Zn–Zn bond center and perpendicular to the long molecular axis. This shows the plot of the ELF torus of the Zn–Zn bond. The cutting plane intersects the ELF value of outer most C–H bonds oriented roughly parallel to the long molecular axis.

at elf = 0.538 the spot and ring emerged to a disk. In contrast to the zincous dication Zn_2^{2+} [7] the Zn–Zn bond basin in $Zn_2Cp_2^*$ is essentially featureless. This is likely a result of the greatly reduced symmetry of the dimetal core surroundings in dizincocene compared to the isolated Zn_2^{2+} ion. The three separate valence regions combine and share a single envelop at approximately elf = 0.200.

In Fig. 8 the projection of the Zn–Zn torus was visible a ring of colour obscured by the green balls (C atoms) and the five C–C bond basins. The center spot is not discernable under the position of the Zn atom in the center of the Fig. 8. Note that the Zn atom was not centrally located with respect to the C_5 ring. Referring to Fig. 8 we found that at approximately elf = 0.944 the point-like attractors of the CH_3–C bond basins appear, positioned on the $C–CH_3$ bond at the mid point. As the elf density decreases they develop as roughly spherical surfaces. At elf = 0.919 the attractors of the C = C basins of the σ-π system of the C_5 rings appear at positions displaced by a few pm above (exterior) and outside the ring of C–C bonds making the C_5 ring. In the calculations reported here these C_5 ring bond attractors were similar but not exactly the same as found for ethylene (point attractors M^1 and M^2 symmetrically above and below the direct C = C axis [9,25]) or benzene (point attractor on the plane but about 5 pm outside the C_6 ring [26]). The asymmetry is evident in Figs. 7 and 8, though it is most clearly seen on isometric surfaces for higher ELF values. These C–C ring basins develop a cylindrical shape and at high ELF values resemble those of calculated for ethylene [9] except the previously mentioned distortion. This observation is consistent with the curvature or dishing of the Cp^* ligands described earlier.

4. Discussion and summary

In this final section we consider: dizincocene crystal structure, molecular geometry, chemical bonding and comment briefly on possible experiments with dizincocene crystals and applications of dizincocene-type molecules.

4.1. Packing in the crystal

Dizincocene forms white triclinic P_1 crystals [1,2] with two molecules in the unit cell related by a centre of symmetry. The Fig. 9 shows some aspects of the crystal structure and molecular packing adapted from the published crystal data [1,2]. Fig. 9A is a wire frame model of the unit cell viewed along the $\langle 0,1,0\rangle$ direction. Fig. 9B shows the view along direction $\langle -1,1,1\rangle$ in which the two inversion symmetry related molecules (A and B) are aligned one behind the other in chains (...ABAB...). These chains have a zigzag appearance when viewed perpendicular to the chain direction because in adjacent molecules Cp^* rings are oppositely tilted.

Fig. 9C is a cartoon of the how the molecules are arrayed in step-like rows when viewed along the $\langle -1,1,1\rangle$ direction. Note that the array has the appearance of an interlocked staircase. As viewed this staircase is deceptive since it exists in three directions, the crystal structure being a compact way packing the "cocktail" glasses in 3D. In a given molecule the top Cp^* lies in the hollow between molecules on a higher step while the lower head forms part of

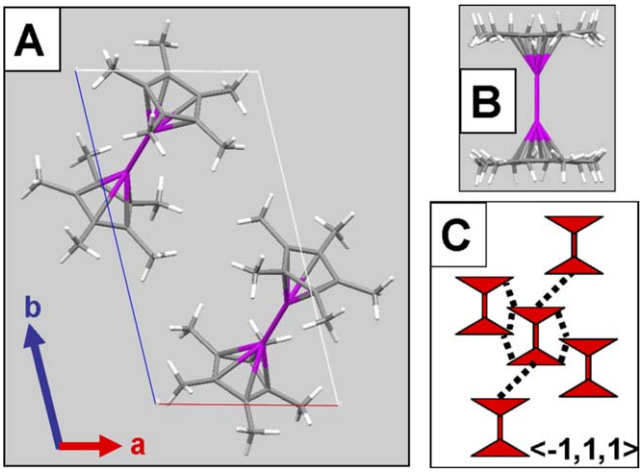

Fig. 9. A shows the triclinic unit cell of crystalline $Zn_2Cp^*_2$ viewed along the $\langle 0\,1\,0\rangle$ direction showing the two molecules related by inversion symmetry. B the view of one unit cell along $\langle -1,1,1\rangle$ showing how the molecules are lined behind one another. C a cartoon depicting the "3D staircase" packing of molecules viewed along the $\langle -1,1,1\rangle$ direction.

the pillow of two head for the third molecule. The interactions of the methyl groups likely dominate the crystal packing energy. This is shown schematically Fig. 9C based on nearest atom overlaps in crystal structure. The packing places a constraint on the extent to which the Cp^* rings can tilt.

4.2. Molecular geometry

The calculations reported here and some previous ones show distortions similar to those seen in the crystal measurements described above. The published crystallographic data [1,2] show distortions away from an eclipsed D_{5h} conformation. Fivefold site symmetry is not possible in 2D and 3D arrays of identical molecules so displacements out of fivefold symmetry are expected. Within a given molecule the two Cp^* rings are not precisely superimposed when viewed along the dizinc axis. The calculations reported here indicate that in the zinc system there is a small tendency for the Cp^* planes to have a small relative tilt and for the nearest metal atom to be unsymmetrically located relative to all five C atoms of the cyclopentadienyl ligand. We do not see a clear propensity for the zinc atoms to bond preferentially to one C atom. However, migration of the metal-Cp^* bonding from central to the edge of the C_5 ring would signal the preference of one ring atom over another. The ELF valence basins of the Cp^* ligand in Figs. 8 and 9 show a differentiation into two different type of bond in the C_5 ring. There are two cylindrical C–C basins resembling C = C basin in ethylene and three that are more egg shaped and so resemble a C–C bond basin. This could happen because of loss of aromatic stabilization of the Cp^* ring due to metal atom size or a preferential localization on a specific ring carbon directed by ring substituents, as might happen with a "notched" ligand like C_5Me_4H [27]. So there are tantalizing hints of a hybridization change in Cp^* as an explanation of the geometrical distortion we have termed "dishing".

4.3. Chemical bonding

The calculated gap between homo-1 and lumo-1 (ca. 3 eV) is large enough for the molecule to be predicted as physically stable. The KS level homo-5 has the largest overlap between zinc atoms and therefore contributes the greatest charge to the Zn–Zn bond. The ELF density between zinc atoms is distinctive and analogous to that found in the zincous dication. The Zn–Zn bond is not just a simple σ-bond arising from 4s to 4s metal orbital overlap, there are small contributions to σ-bonding from functions p_z and d_{z^2} even inside a sphere 115 pm in diameter. There is also a weak π-electron contribution to the overall bond from zinc d_{zx}- and d_{yz}-functions. The latter also participate in "over-the-top" π-bonding overlap with p_z-functions on the Cp^* rings. The Zn–Cp^* chemical bond exhibits extensive overlap between various d_{zx}- and d_{yz}-functions on zinc in combination with 4s-, $4p_x$- and $4p_y$-functions which shrink the metal lobes in closest to the Cp^* ring.

4.4. Molecular electronics

The geometry of the molecule makes it an interesting test bed for components in molecular electronics. The confinement of the lumo charge in between the Cp^* ligands suggest novel applications, though not within the triclinic structure. Most aromatic chromophores are two-dimensional with π–π^* transitions exposed to neighbours [28]. In dizincocene the transition is buried. Based on simple overlap considerations, the lowest $\sigma - \pi^*$ transition in the zinc core should correspond to a singlet molecular exciton state. The confinement of the excitation by the Cp^* rings suggests new materials for energy and electron transfer provided by multi-metalocenes with polycyclic aromatic ligands. Finally, much more work remains to be done on this unusual system. In particular more detailed understanding of the electron density using ELF and the tools associated with atoms-in-molecules analysis [9,29].

Acknowledgements

MRP acknowledges the partial support of the Academic Research Fund of the National University of Singapore 2004–05, the provision of a long term visiting professorship 2004-05 by the Japan Society for the Promotion of Science, and the hospitality of the Center for Computational Materials Science, IMR-Tohoku University where all this work was done. The authors also express their thanks to the staff of the Center for Computational Materials Science of the Institute for Materials Research, Tohoku University for their dedicated and enthusiastic support of the SR8000 supercomputing facilities.

References

[1] I. Resa, E. Carmona, E. Gutierrez-Puebla, A. Monge, Decamethyldizincocene a stable compound of Zn(I) with a Zn–Zn bond, Science 305 (2004) 1136.
[2] D. Del Rio, A. Galindo, I. Resa, E. Carmona, Angew. Chem. Int. Ed. 44 (2005) 1244.
[3] W.G. Wyckoff, second ed.Crystal Structures, vol. I, Interscience, NY, 1965, p. 111.
[4] F.A. Cotton, G. Wilkinson, C.A. Murilo, M. Bochmann, Advanced Inorganic Chemistry, sixth ed., Wiley, NY, 1999, p. 598 (Chapter 15).
[5] M. Kaupp, H.G. von Schnering, Inorg. Chem. 33 (1994) 2555.
[6] H.-J. Flad, F. Schautz, Y. Wang, M. Dolg, A. Savin, Eur. Phys. J. D 6 (1999) 243.
[7] M.R. Philpott, Y. Kawazoe, The electronic structure of the dizincocene core, Chem. Phys. (2006) in press.
[8] A.D. Becke, K.E. Edgcombe, J.Chem. Phys. 92 (1990) 5397.
[9] B. Silvi, A. Savin, Nature 371 (1995) 683.
[10] Y. Xie, H.F. Schaefer III, E.D. Jemmis, Chem. Phys. Lett. 402 (2005) 414.
[11] Z.-Z. Xie, W.-H. Fang, Chem. Phys. Lett. 404 (2005) 212.
[12] Y. Xie, H.F. Schaefer III, R. Bruce King, J. Am. Chem. Soc. 127 (2005) 2818.
[13] H.S. Kang, J. Phys. Chem. A 109 (2005) 4342.
[14] J.W. Kress, J. Phys. Chem. A 109 (2005) 7757.
[15] A.Y. Timoshkin, H.F. Schaefer III, Organometallics 24 (2005) 3343.
[16] S.L. Richardson, T. Baruah, M.R. Pederson, Chem. Phys. Lett. 415 (2005) 141.
[17] J.P. Perdew, Unified theory of exchange and correlation beyond the local density approximation, in: P. Ziesche, H. Eschrig (Eds.), Electronic Structure of Solids 1991, Akademie-Verlag, Berlin, 1991.
[18] J.P. Perdew, J.A. Chevary, S.H. Vosk, K.A. Jackson, M.R. Pederson, D.J. Shingh, C. Fiolhais, Phys. Rev. B 46 (1992) 6671.
[19] D. Vanderbilt, Phys. Rev. B 41 (1990) 7892.
[20] G. Kresse, J. Halfner, Phys. Rev. B 47 (1993) 588.
[21] G. Kresse, J. Halfner, Phys. Rev. B 49 (1994) 14251.
[22] G. Kresse, J. Furthmuller, Comput. Mater. Sci. 6 (1996) 15.
[23] G. Kresse, J. Furthmuller, Phys. Rev. B 54 (1996) 11169.
[24] M.R. Philpott, Y. Kawazoe, unpublished calculations for Zn_2L_2 molecules, 2005.
[25] H. Grützmacher, T.F. Fässler, Chem. Eur. J. 6 (2000) 2317.
[26] M.R. Philpott, Y. Kawazoe, unpublished organic molecule ELF calculations, 2005.
[27] J.A. Pool, E. Lobkovsky, P.J. Chirik, Nature 427 (2004) 527.
[28] M.R. Philpott, Some Modern Aspects of Exciton Theory, Adv. Chem. Phys. 23 (1973) 227–341.
[29] R.F.W. Bader, Atoms in Molecules: A Quantum Theory, Clarendon Press, Oxford, 1990.